Journal of the European Ceramic Society 7 (1991) 135–145

Unlubricated Sliding Behaviour of Various Zirconia-based Ceramics

M. Woydt,[a] J. Kadoori,[b] K.-H. Habig[a] & H. Hausner[b]

[a] BAM, Federal Institute for Materials Research and Testing, Div. 5.2, Unter den Eichen 87, W-1000 Berlin 45, FRG

[b] Technical University of Berlin (Sekr. ES3), Englische Straße 20, W-1000 Berlin 12, FRG

(Received 12 February 1990; revised version received 16 March 1990; accepted 2 July 1990)

Abstract

The unlubricated sliding friction and wear behaviour of self-mated sliding couples of 2, 3, 6, and 8 mol% Y_2O_3/ZrO_2 and of 3·3 wt% MgO/ZrO_2 were studied at 22°C and up to 1000°C ambient temperature in the sliding-speed range from 0·03 m/s up to 3 m/s. The morphologies of the worn surfaces and of the wear debris were studied by means of SEM, XRD, and TEM. The phase composition and the mechanical and physical properties of these ceramics are presented to find a potential correlation between these properties and the observed tribological behaviour. To understand the phenomena, additional hot-spot-temperature calculations and simulations were made.

Das artgleiche Verschleiß- und Gleitreibungsverhalten der fünf Werkstoffe x Mol.% Y_2O_3/ZrO_2 ($x = 2, 3, 6$ und 8) bzw. 3·3 Gew.% MgO/ZrO_2 wurde ohne Schmierung im Temperaturbereich von 22°C bis 1000°C und im Geschwindigkeitsbereich von 0·03 m/s bis 3 m/s untersucht. Die Morphologie der beanspruchten Oberflächen und des Abriebs wurde mit Hilfe des REM, des TEM und der Röntgenbeugung beurteilt. Auf den Zusammenhang der Phasenzusammensetzung, der mechanischen und der physikalischen Eigenschaften dieser Keramiken mit dem gefundenen tribologischen Verhalten wird eingegangen. Um die beobachteten Phänomene zu verstehen, wurden zusätzliche Berechnungen und Simulationen lokaler Temperaturspitzen durchgeführt.

On a étudié le comportement en frottement par glissement non lubrifié et la résistance à l'usure de couples de glissement auto-apparié de Y_2O_3/ZrO_2 (teneurs en Y_2O_3: 2, 3, 6 et 8% molaires) et de 3·3% massiques de MgO/ZrO_2 à des températures ambientes entre 22 et 1000°C et pour des vitesses variant de 0,03 à 3 m/s. La morphologie des surfaces usées et des débris d'usure a été étudiée par microscopie à transmission et à balayage ainsi que par diffraction X. On donne ici la composition des phases et les valeurs des propriétés physiques et mécaniques dans le but d'établir une relation entre ces propriétés et le comportement tribologique observé. On a également effectué des calculs de températures de zone de surchauffe et des simulations permettant de comprendre le phénomène.

1 Introduction

Mechanical systems subjected to wear can be broadly classified as open and closed tribological systems. Open tribological systems are systems in which the wear of one triboelement is of no major concern, as, for instance, the workpiece in the tribosystem 'tool–workpiece'. In closed tribological systems, both triboelements are in contact and overlap in a specific ratio, and the wear of both triboelements is of importance. Closed tribological systems exchange energy, but no matter is exchanged with the environment.

In open tribological systems, the wear of the counterbody is negligible. By using a ceramic material instead of a metal, the lifetime and reliability can increase considerably, thus creating the frame of improved ceramic performance, which cannot be taken for granted in closed tribological systems.[1,2]

A significant part of the materials development in the field of advanced ceramics is related to the improvement of the mechanical properties. It should be remembered, however, that the tribological behaviour is the result of the reaction of interacting surfaces in relative motion under given operating

Journal of the European Ceramic Society 0955-2219/91/$3.50

variables. No strict correlation between mechanical and tribological properties exists.

The tribological behaviour of many ceramic–ceramic sliding couples is not known precisely and requires further research.

2 Previous work

Winer *et al.*[3] have shown for HPSN–sapphire wear couples that the Si_3N_4-pin can reach, in unlubricated sliding conditions at 1·5 m/s and 8·9 N, 'hot-spot' temperatures of 2100 K. Temperatures of the same order of magnitude can occur in the contact surface of $MgO–ZrO_2/MgO–ZrO_2$ sliding couples so that a phase transformation into the high-temperature cubic modification is possible. The formation of cubic-ZrO_2 by unlubricated sliding of zirconia was also found by Yust.[4] He analysed the structure of the wear debris that had accumulated in surface pores by electron diffraction. The diffraction pattern of selected areas demonstrated the presence of cubic zirconia. No monoclinic or tetragonal phase could be observed.

A network of cracks was found on aerodynamic $MgO–ZrO_2$ bearing shells after 3000 starts and stops at a temperature of 600°C.[6] In application-oriented tests, an important influence of the sliding speed on the volumetric wear coefficient of $MgO–ZrO_2$ bearing shells sliding against an $HP–Si_3N_4$ journal was observed. Up to 5 m/s, the wear of the $MgO–ZrO_2$ shell increased by more than several orders of magnitude. With aerodynamic lubrication introduced the shell wear decreased.[6]

New results by Fischer *et al.*[7] show that the tetragonal ZrO_2 has a higher wear resistance, which is 2·5 orders of magnitude higher than that of cubic ZrO_2. The tests by Fischer *et al.* were conducted in a pin-on-disc test rig at 9·8 N and 1 mm/s in different ambient media with three ceramic materials:

(a) 6·0 mol% $Y_2O_3–ZrO_2$ (cubic, $k_{IC} = 2{\cdot}5\ MPa\ m^{1/2}$)
(b) 3·0 mol% Y_2O_3-ZrO_2 (tetragonal, $k_{IC} = 11{\cdot}6\ MPa\ m^{1/2}$)
(c) 4·0 mol% $Y_2O_3–ZrO_2$ (50 v% tetragonal, 50 v% cubic, $k_{IC} = 8{\cdot}7\ MPa\ m^{1/2}$)

Gane and Breadsley[8] observed under unlubricated sliding conditions ($v = 0{\cdot}47$ m/s, $F_N = 5$ N) that the wear of a fully stabilized ZrO_2 pin (cubic) sliding on a PSZ disc is 20 times as high as that of a PSZ pin sliding on a PSZ disc. The wear of a PSZ pin depends extremely critically on the applied load. Increasing the load from 5 N to 55 N raises the PSZ pin-wear coefficient by a factor of 380.

3 Experimental

3.1 Tribometer

The high-temperature test rig used in this study has been described in detail elsewhere.[9,10] The operating conditions are detailed in Table 1. The tribological behaviour of a commercial $MgO–ZrO_2$ (PSZ) up to 1000°C and that of $2Y_2O_3–ZrO_2$ (PSZ), $3Y_2O_3–ZrO_2$ (PSZ), $6Y_2O_3–ZrO_2$ (CSZ), and $8Y_2O_3–ZrO_2$ (CSZ) at room temperature has been investigated. The properties of the materials are summarized in Table 2.

3.2 Unlubricated sliding of self-mated $MgO–ZrO_2$ couples

3.2.1 Material characteristics

The partially stabilized ZrO_2 (ZN40, Feldmühle AG, 3·3 weight% MgO) has a uniform distribution of 40–50% of tetragonal ZrO_2 and 5% of the monoclinic phase in a cubic–ZrO_2 matrix.[11]

3.2.1.1 Surface roughness. The surface roughness R_z(C.L.A) and R_z of the rotating disc were measured at four points of each sample. The average C.L.A value of all samples was $0{\cdot}028 \pm 0{\cdot}01\ \mu m$ and the R_z-value $0{\cdot}58 \pm 0{\cdot}13\ \mu m$. The samples were polished to exclude any influence of the surface roughness.

Table 1. Operating variable of the high-temperature test rig (HT1)

Tribosystem parameters	*Specifications*
Type of motion	Continuous sliding
Normal force	1–20 N
Sliding velocity	0·02–5 m/s
Temperature	22–1000°C (1200°C)
Element 1	Pin
Element 2	Disc (42 mm 0)
Interfacial medium	None
Surrounding atmosphere	Air
Wear mechanisms	Abrasion, adhesion, tribo-oxidation
Friction force	f (continuously)
Total linear wear rate	W_1 (continuously)
Temperature sample	T_s (continuously)
Morphology of the worn surfaces	
Composition of the wear particles	

Table 2. Mechanical and physical properties and phase composition of ZrO_2 materials used at 22 °C

ZrO_2 material	E N/mm^2	$\sigma 4dB$ MPa 22 °C	$\sigma 4dB$ MPa 800 °C	K_{Ic} $MPa\,m^{1/2}$ at 22 °C	λ $W/(m*K)$	C_p $J/(g*K)$	α RT-1000 °C $10^{-6}/k$	HV 0·2 GPa	R_a μm	R_z μm	Phase composition (%) mono.	tetra.	cubic
3,3 w/o MgO[a] (ZN40)	210·000[a]	520[a]		8·1[a]	2·1[a]	0·4[a]	9·8[a]	11 080 ± 610[c]	0·028 ± 0·1[c]	0·58 ± 0·23[c]	8	52	40
2 mol.-% Y_2O_3[b] (2Y-PSZ)	199·000	716[b]	270[b]	8·3[b]			11·3[b]	12 840 ± 400[c]	0·056 ± 0·016[c]	0·9 ± 0·2[c]	26	67	7
3 mol.-% Y_2O_3 (3Y-PSZ)	204·000	633[b]	241[b]	9·5[b]			11·1[b]	13 740 ± 600[c]	0·045 ± 0·005[c]	0·9 ± 0·2[c]	16	74	10
6 mol.-% Y_2O_3[b] (6Y-CSZ)	195·000	232[b]		2·4[b]			10·6[b]	12 500 ± 700[c]	0·1 ± 0·005[c]	0·6 ± 0·1[c]	0·3	0	99·7
8 mol.-% Y_2O_3[b] (8Y-CSZ)		220[b]		2·4[b]	2·2		10·5[b]	13 500 ± 500[c]	0·1 ± 0·005[c]	0·6 ± 0·1[c]	0	0	100·0

[a] Feldmühle AG. Prospectdatas.
[b] TU Berlin, Prof. Hausner.
[c] BAM-5.24. Berlin.

3.2.1.2 Microstructure. From the etched micrograph in Fig. 1, an average grain size of 80–90 μm and a pore size of 3–6 μm were determined.

3.2.1.3 Hardness. The HV 0·2 Vickers hardness was 11 080 MPa. Around the indentation, plastic deformation with shear bands occurred. The Vickers-indentation technique therefore has to be used with caution in making fracture-toughness measurements.

3.2.2 Coefficient of friction

The friction coefficients of the couple $MgO–ZrO_2$/$MgO–ZrO_2$ are always greater than 0·4 after a sliding distance of 1000 m (Fig. 2). The high values are caused by 'wear-particle adhesion' on the sliding surfaces. These wear particles are a resistance against sliding. Above 0·3 m/s, the coefficient of friction decreases with increasing temperature and sliding velocity.

The coefficient of friction of self-mated couples of $MgO–ZrO_2$/$MgO–ZrO_2$ can reach low values of 0·1 after 10 m at room temperature (Fig. 2). This indicates that, for tribological tests, a sufficient sliding distance is necessary in order to achieve steady-state conditions.

These results demonstrate why ceramics have been considered to be low-friction materials after results had been reported in the literature that had been obtained under low-speed and short-test-time conditions.

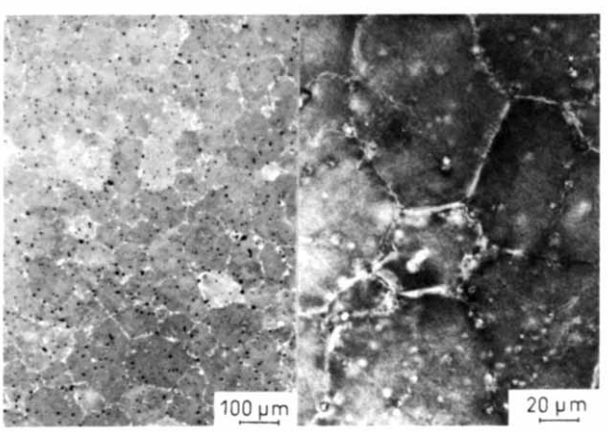

Fig. 1. Microstructure of $MgO–ZrO_2$ (PSZ; ZN40).

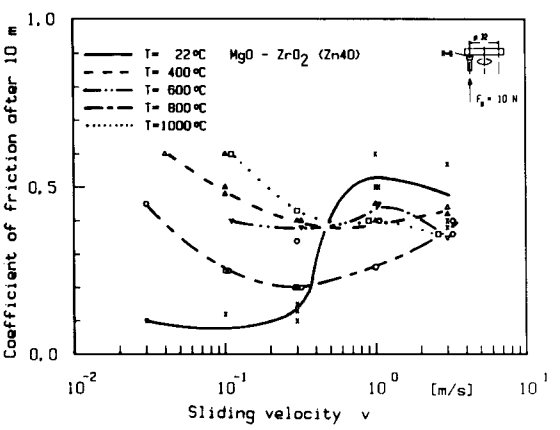

(a)

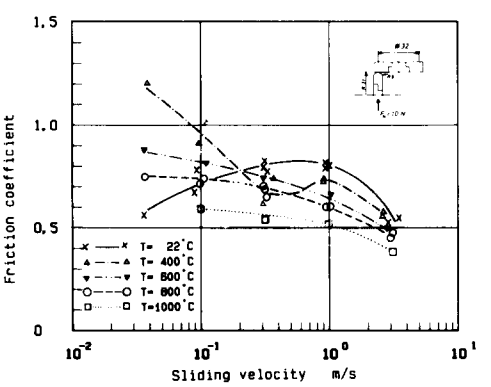

(b)

Fig. 2. Coefficient of friction as a function of sliding velocity at different temperatures of self-mated $MgO–ZrO_2$-couples after (a) 10 m and (b) 1000 m under unlubricated sliding conditions.

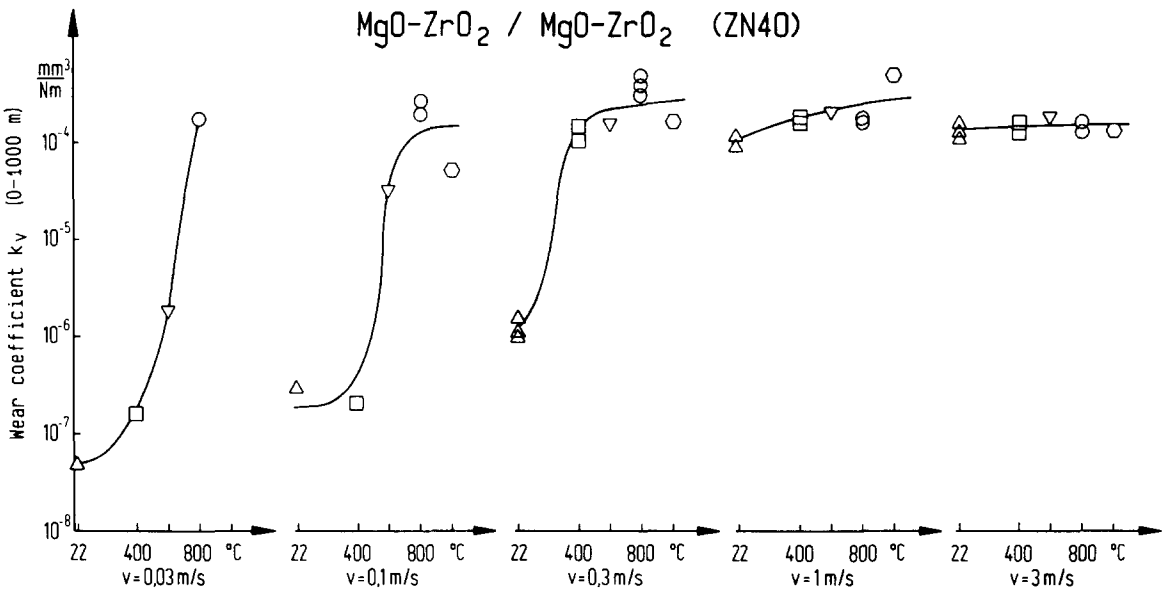

Fig. 3. Total volumetric wear coefficient k_v of self-mated $MgO–ZrO_2$ sliding couples as a function of sliding speed at different ambient temperatures under unlubricated conditions.[5]

3.2.3 Wear coefficient

The volumetric wear coefficient can be calculated by dividing the wear volume by the normal force of 10 N and the constant sliding distance of 1000 m.

3.2.3.1 Total wear coefficient. Figure 3 shows the total wear coefficient of stationary and rotating specimens of the couple $MgO–ZrO_2/MgO–ZrO_2$ plotted as a function of temperature at different sliding speeds. At room temperature and 400°C, with sliding velocities smaller than 0·3 m/s, the wear behaviour is interesting for unlubricated applications as the coefficient k_v is less than 10^{-6} mm^3/N m.

In the speed range between 0·3 and 3 m/s, the sliding velocity has a strong influence on wear, which increases from a low-wear regime to a high-wear regime.

At 800°C and 1000°C, wear is in the high region and is only slightly dependent on the sliding velocity. The results show that, for self-mated wear couples of $MgO–ZrO_2/MgO–ZrO_2$, the influence of temperature on the wear behaviour can be simulated by changing the sliding speed, since frictional heating is enhanced by an increase in the sliding velocity.

3.2.3.2 Wear of the stationary specimen. In Fig. 4, the pressure that is present during the transition from the high-wear to the low-wear region is plotted as a function of sliding velocity. With increasing sliding velocity, the pressure decreases. At 400°C, 800°C, and 1000°C, the wear volume of the stationary specimen is independent of surface pressure without a transition to low wear.

3.2.3.3 Wear volume of the stationary and rotating specimens. The different contributions of the stationary and rotating specimens to the total wear volume are shown in Fig. 5. It can be seen that the low-wear/high-wear transition of the rotating specimen (disc) occurs at 0·3 m/s, whereas the stationary specimen reaches this transition at a higher velocity of 3 m/s (see Section 4).

3.2.4 Morphology of worn surfaces

The surface morphology of the low-wear region is characterized by some grooves formed by running-in abrasion (Fig. 6a). At 400°C, the surface becomes roughened owing to plastic deformation and wear-particle adhesion (Fig. 6b). Cracking, probably

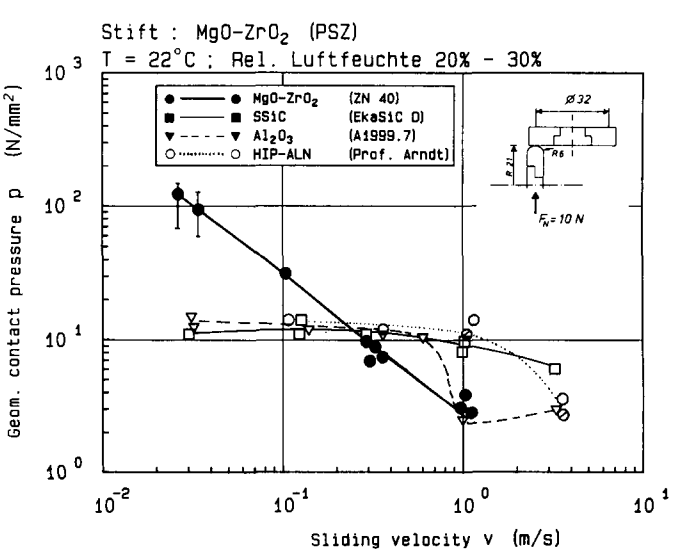

Fig. 4. Geometric surface pressure as a function of sliding velocity for the high-wear/low-wear transition under unlubricated sliding conditions.

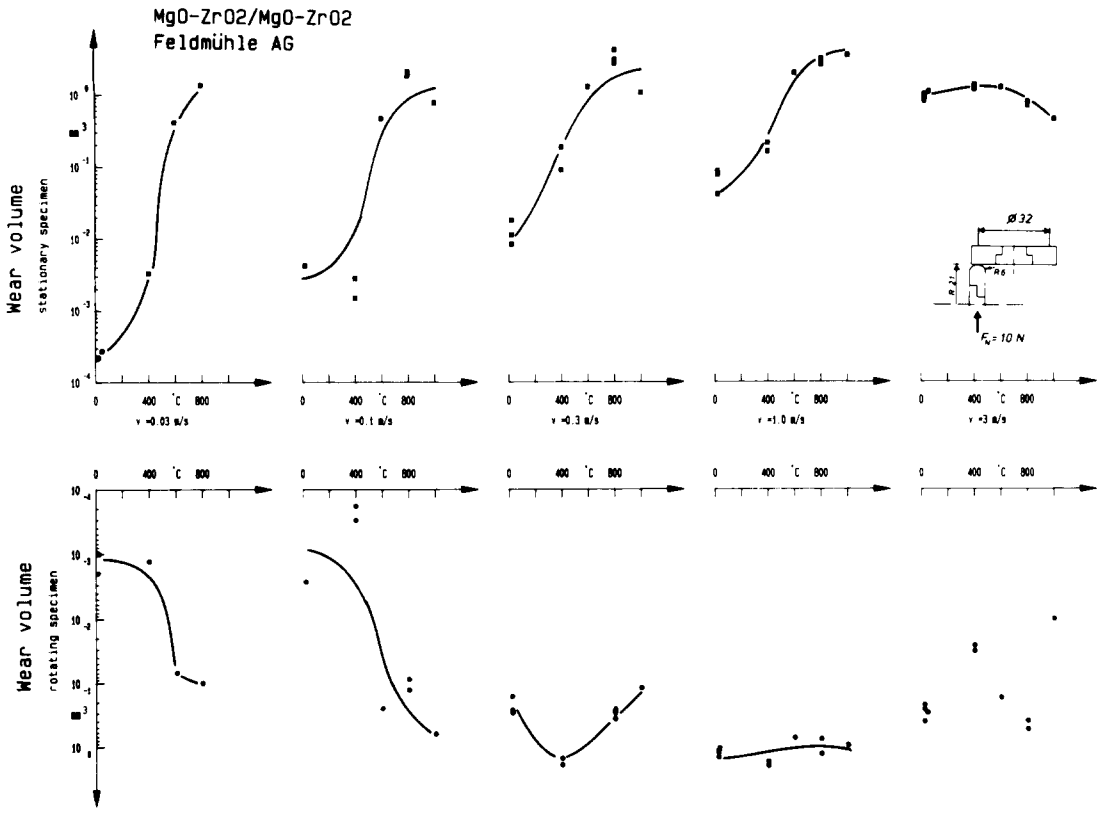

Fig. 5. Wear volume of pin and disc of $MgO–ZrO_2/MgO–ZrO_2$ sliding couples as a function of sliding speed at different ambient temperature.

along grain boundaries, occurs at high sliding speeds (Fig. 6c).

Wear-particle adhesion is the predominating 'wear mechanism' in the high-wear region.

3.2.5 Friction-induced phase transformations

In the system $MgO–ZrO_2$, different phases exist depending on temperature and stabilizer concentration. At room temperature, the monoclinic phase is stable. At 900–1000°C, a transformation to the tetragonal phase occurs, and, with a further increase of temperature, the cubic phase becomes stable with a decrease in the crystallographic volume up to 8 vol%. The low-wear–high-wear transition of $MgO–ZrO_2$ may be related to phase transitions of the original material. The X-ray-diffraction analysis of wear particles and disc-wear scars resulting from tests in the high-wear regime showed only cubic ZrO_2 (Table 3). The results obtained by X-ray diffraction were confirmed by TEM analysis of wear particles. The electron-diffraction pattern does not show monoclinic rings or the 10%-(002)-tetragonal ring.[10,22] Similar results were found by Yust *et al.*[4,5]

Table 3. Characteristics of ZrO_2 (Y_2O_3) Samples

Composition	*Grain size* (μm)	*Flexural strength,* S_0 (*Weibull*) (MPa)	k_{IC} ($MPa\,m^{1/2}$)
ZrO_2 ($2Y_2O_3$)	0·1–0·3	720	8·3
ZrO_2 ($3Y_2O_3$)	0·1–0·3	630	9·5
ZrO_2 ($6Y_2O_3$)	1–3	230	2·4
ZrO_2 ($8Y_2O_3$)	1–5	220	2·4

3.2.6 Calculation of the hot-spot temperature

The hot-spot temperature of two flat $MgO–ZrO_2$ bodies sliding on each other at 0·03 m/s and 3 m/s was evaluated by Kuhlmann-Wilsdorf and Makkel,[15] using a theoretical model.[16] The main inputs in this micro-contact model are:

the frictional heat is evolved at mathematically flat surfaces, the two materials are free of surface films, the two materials have the same bulk temperatures, and data for temperature-dependent material were used.

Figure 7 presents the flash temperature as a function of ambient temperature and the number of micro-contacts. Under these test and material conditions, a value of 10 micro-contacts can be assumed from the results of Winer,[12,17] which gives a flash temperature in Fig. 7 of about 2200°C above ambient temperature.

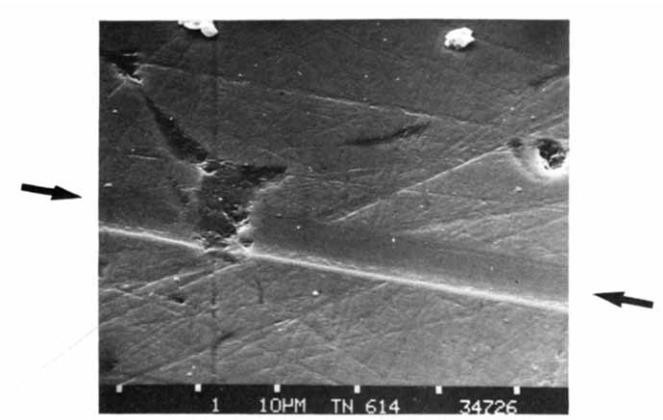

Fig. 6a. Morphology of a worn disc under solid-state friction ($F_N = 10$ N; $v = 0{\cdot}03$ m/s; $T = 22°C$; $s = 940$ m).

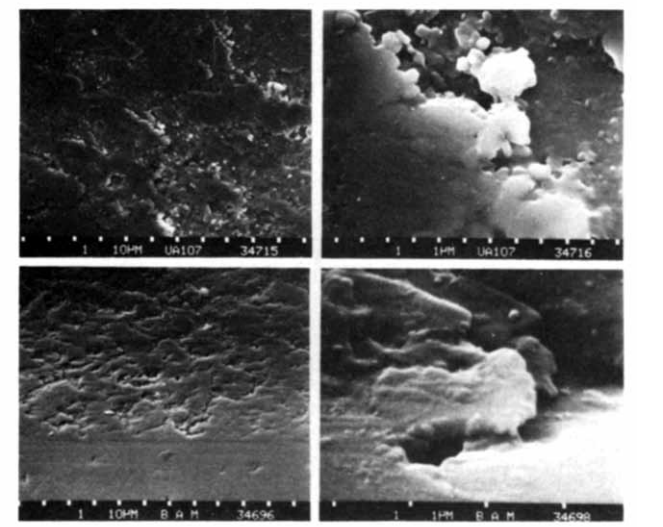

Fig. 6b. Morphology of a worn disc and pin under solid-state friction ($F_N = 10$ N; $v = 0{\cdot}04$ m/s; $T = 400°C$; $s = 1100$ m).

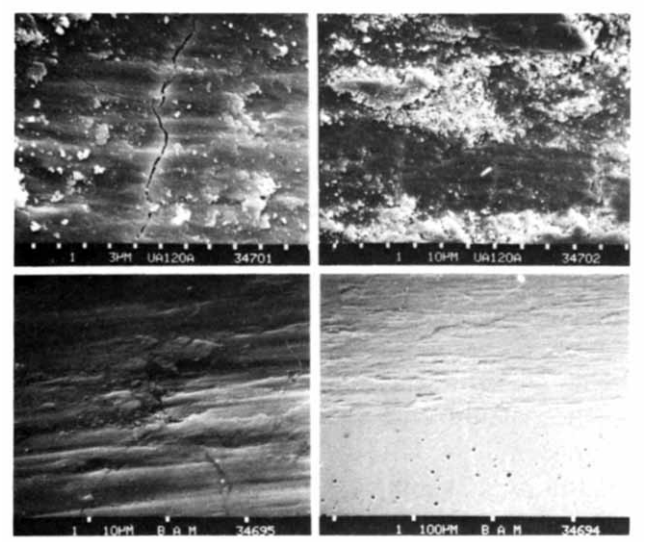

Fig. 6c. Morphology of a worn pin and disc under solid-state friction ($F_N = 10$ N; $v = 3{\cdot}3$ m/s; $T = 22°C$; $s = 1190$ m).

3.3 Unlubricated sliding of self-mated Y_2O_3–ZrO_2 couples

From the tribological results with MgO–ZrO_2, the question arises of whether the thermo-mechanical response of the ZrO_2 surface to the frictional heat can be moderated or suppressed by using ZrO_2 materials with different amounts of monoclinic, tetragonal, and cubic phases. In this investigation, only tests with a variation in the sliding velocity at 22°C were necessary because the low-wear–high-wear transition with increasing ambient temperature can also be realized by an increase in speed. The hot-spot temperature is the sum of the flash and ambient temperatures. With increasing ambient temperature and sliding speed (see Section 3.2.6) the tetragonal–cubic transition temperature is reached more quickly.

3.3.1 Material characteristics

In the system ZrO_2–Y_2O_3, four compositions were investigated: ZrO_2 ($2Y_2O_3$), ZrO_2 ($3Y_2O_3$), ZrO_2 ($6Y_2O_3$), and ZrO_2 ($8Y_2O_3$). From the powders (Tosoh Corp.), specimens were prepared by dry-pressing with dimensions $60 \times 60 \times 12$ mm and sintered at 1350°C to densities between 96 and 98% th.d. From these plates, the specimens for the tribological experiments were prepared with diamond drills. The flexural strength and the fracture toughness of the materials were determined in four-point bending with sample dimensions of $50 \times 4 \times 3{\cdot}3$ mm. Microstructural characteristics and mechanical properties at room temperature are shown in Tables 2 and 3.

3.3.1.1 Surface roughness. On each rotating sample, the surface roughness R_z (C.L.A) and R_z were measured at four positions. For the 2-mol% Y_2O_3–ZrO_2 (PSZ) and 3-mol% Y_2O_3–ZrO_2 (PSZ), the average roughness C.L.A was $0{\cdot}05 \pm 0{\cdot}01$ μm and R_z $0{\cdot}6 \pm 0{\cdot}02$ μm, and, for the 6-mol.% Y_2O_3–ZrO_2 (CSZ) and 8-mol% Y_2O_3–ZrO_2 (CSZ) the average roughness C.L.A was $0{\cdot}1 \pm 0{\cdot}02$ μm and R_z $0{\cdot}8 \pm 0{\cdot}3$ μm.

3.3.1.2 Microstructure. The microstructure of the specimens is shown in Fig. 8.

3.3.1.3 Hardness. The HV0·2 Vickers-hardness values are shown in Table 2.

3.3.2 Coefficient of friction

The coefficient of friction after a sliding distance of 10 m self-mated Y_2O_3–ZrO_2 sliding couples are similar to those of the MgO–ZrO_2 sliding couples.

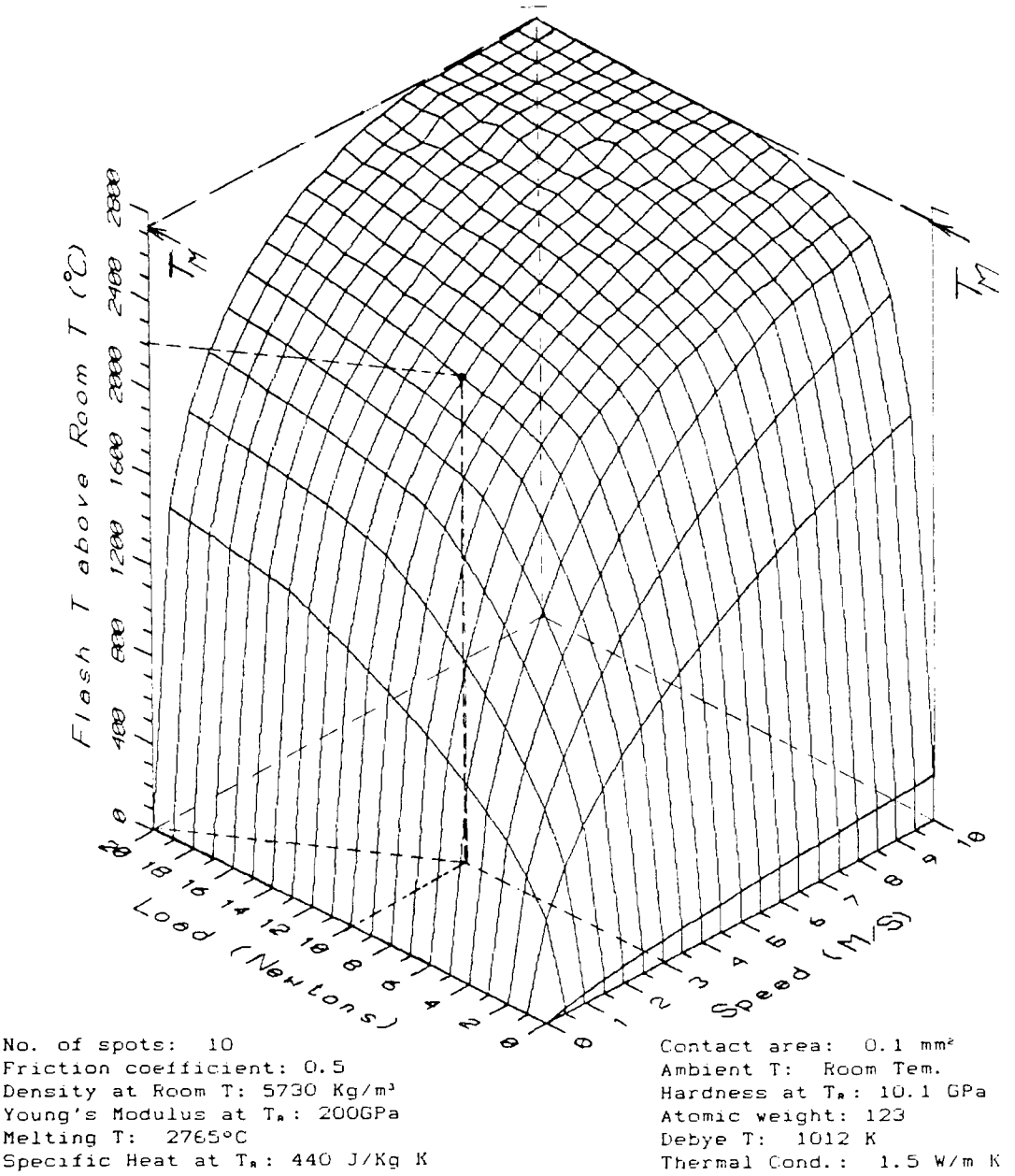

Fig. 7. Calculated flash temperature at 3 m/s of self-mated MgO–ZrO_2 sliding couples (run of 27 April 1989).[15]

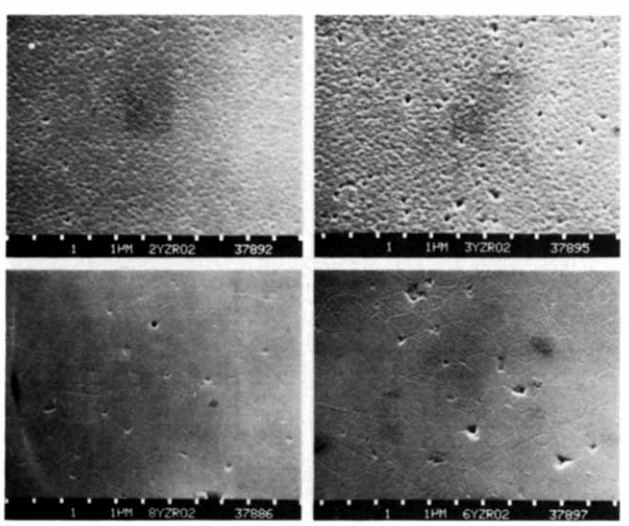

Fig. 8. SEM-graphs of the microstructure of etched Y_2O_3–ZrO_2 materials.

Up to 1 m/s, the measured coefficient of friction is lower than 0·5 and increases with increasing speed (Fig. 9). The steady state coefficient of friction after 1000 m is in excess at 0·5. The cubic ZrO_2 couples have a friction maximum at 0·4 m/s. For the $2Y$–ZrO_2 material a friction maximum was found at 0·2 m/s (Fig. 9).

3.3.3 Wear coefficient

3.3.3.1 Total wear coefficient. The total volumetric-wear coefficient of the Y_2O_3–ZrO_2 sliding couples in Fig. 10 shows a sharper low-wear–high-wear transition with increasing speed. This transition is sharper for the tetragonal material. The speed at which the low-wear–high-wear transition occurs is given in Table 4.

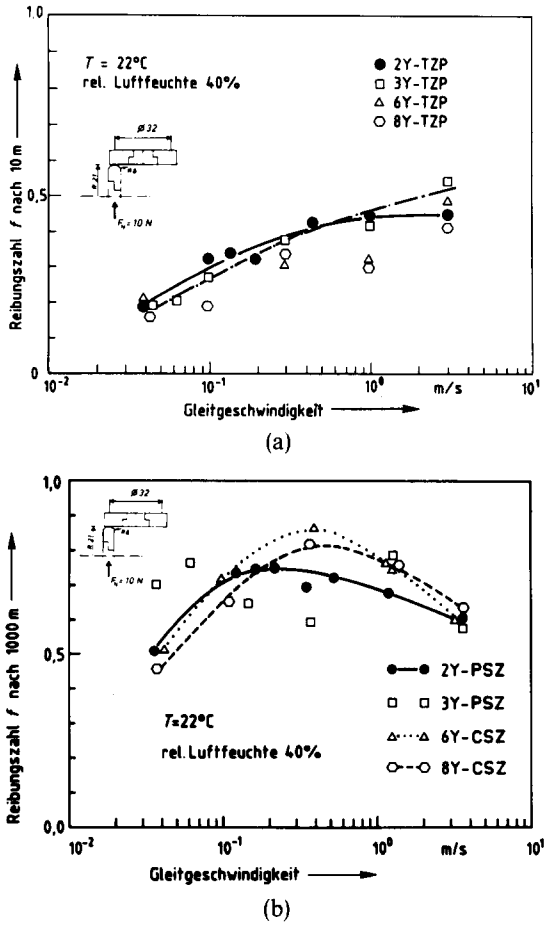

Fig. 9. Coefficient of friction as a function of sliding velocity of different self-mated Y_2O_3 materials at 22°C (a) after 10 m, and (b) after 1000 m under unlubricated sliding conditions.

Table 4. Speed for Lower-wear–High-wear transition

Material	*Transition speed (m/s)*
ZrO_2 ($2Y_2O_3$)	0·14
ZrO_2 ($3Y_2O_3$)	0·08
ZrO_2 ($6Y_2O_3$)	0·04
ZrO_2 ($8Y_2O_3$)	0·04

3.3.3.2 Wear volume of the stationary and rotating specimen. The wear for pin and disc is shown in Fig. 11. The contribution of the stationary and rotating specimens to the low-wear–high-wear transition can be seen.

With the exception of ZrO_2 ($2Y_2O_3$), the disc wear of all Y_2O_3-doped ZrO_2 ceramics comes into the high-wear region at a speed of 0·1 m/s. In the high-wear region, no difference between the different Y_2O_3–ZrO_2 materials could be detected. The ranking of the stationary specimen for the low-wear–high-wear transition is: 2Y–ZrO_2, 3Y–ZrO_2, 6Y–ZrO_2 and 8Y–ZrO_2.

The cubic materials reach the high-wear region at 3 m/s.

3.3.4 Morphology of worn surfaces

In the low-wear region, the wear mechanisms of the Y_2O_3–ZrO_2 sliding couples (Fig. 12a) are identical with those of the MgO–ZrO_2 sliding couples and are characterized by running-in wear grooves and

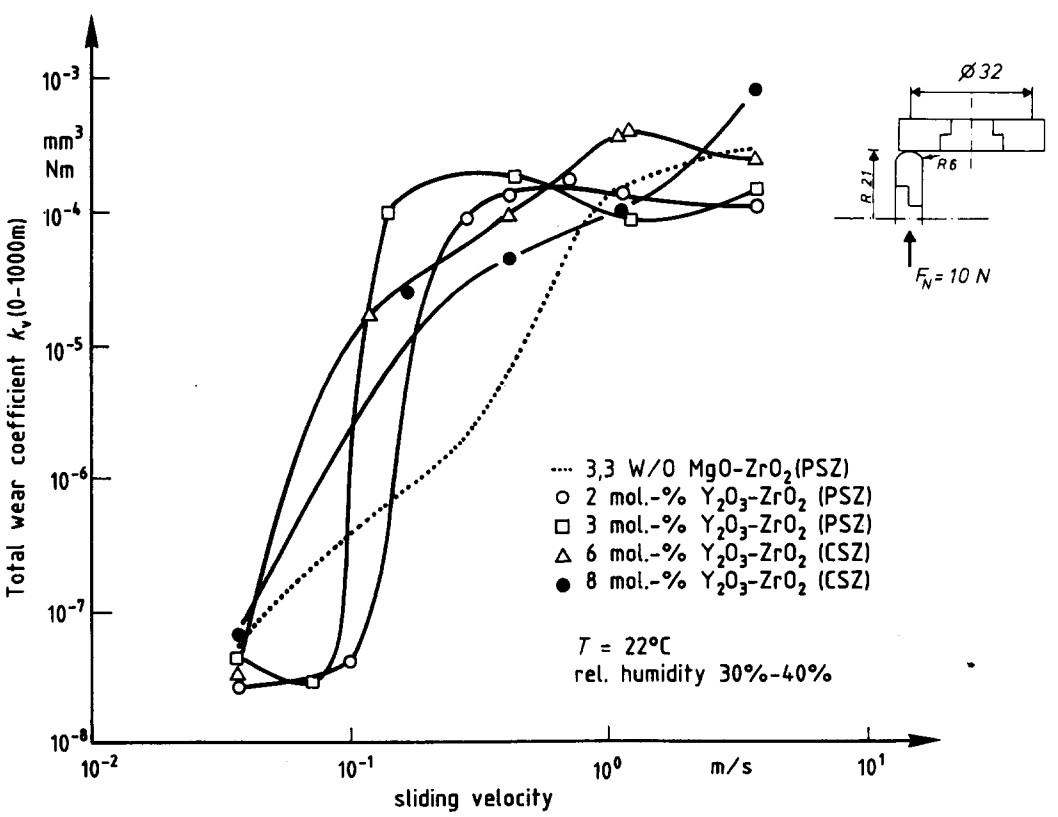

Fig. 10. Total volumetric wear coefficient of self-mated Y_2O_3–ZrO_2 sliding couples under solid-state friction.

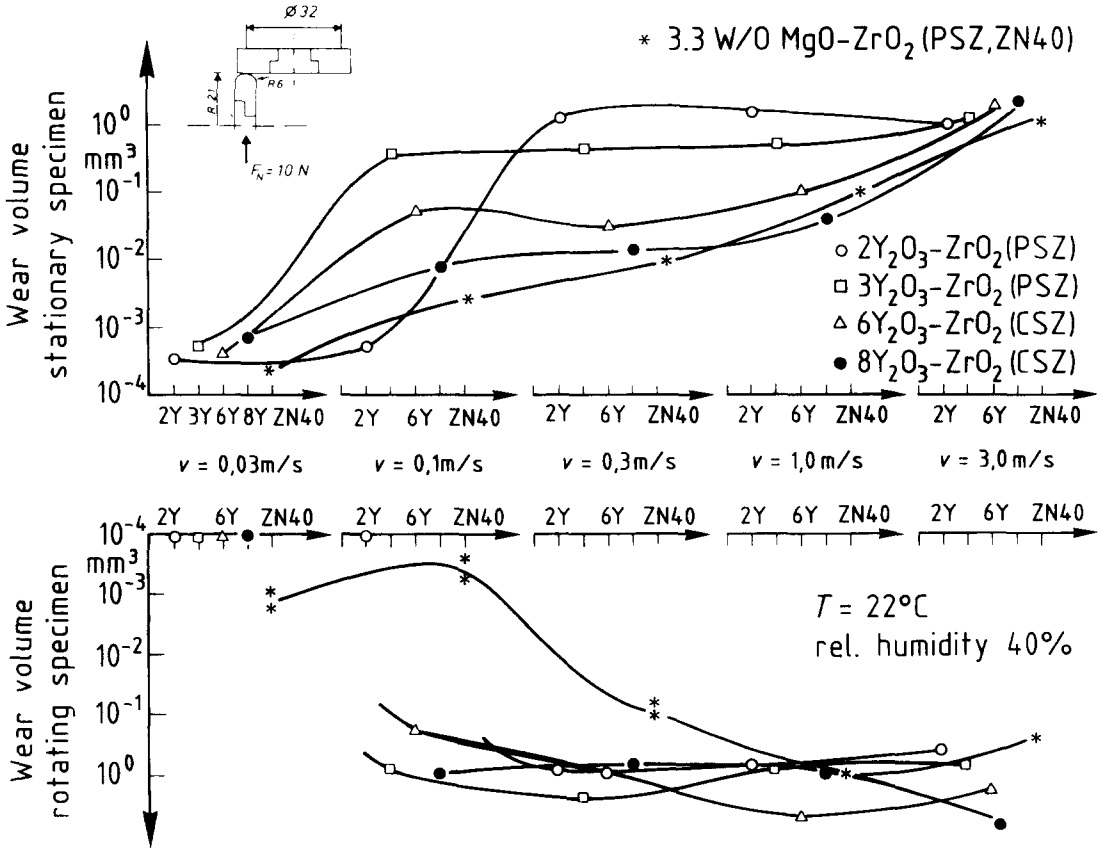

Fig. 11. Wear volume of pin and disc of self-mated ZrO_2 couples as a function of sliding velocity under unlubricated conditions after 1000 m.

polishing. Wear-particle adhesion and roughening by plastic deformation are pronounced for all Y_2O_3–ZrO_2 sliding couples in the high-wear region in the same manner as for the MgO–ZrO_2 sliding couples (Fig. 12b).

4 Discussion of the wear of ZrO_2

The tribological behaviour of self-mated zirconia sliding couples is governed at first by a low-wear–high-wear transition with increasing sliding speed and ambient temperature. The different mechanisms of this transition are described below.

4.1 High wear

The magnitude of wear depends on the applied tribological stress and the possible reaction, based on the physical and chemical properties of the sliding surfaces, to these stresses.

Stresses can be created by:

(a) point and cyclic-sliding-contact pressure,
(b) cyclic, thermal dilatation, and
(c) phase transitions.

4.1.1 Thermal dilation

The physical properties of the three ZrO_2 phases are very similar. The cyclic, thermal dilation due to the frictional heating is nearly the same.

4.1.2 Phase transition

At the high, frictional hot-spot temperatures at higher sliding speeds in conjunction with the micro-asperity pressure (up to 60 GPa), all initial monoclinic and tetragonal-phase transitions to the cubic phase leads to surface stresses and cracks (see Fig. 6c and Fig. 7).[22] The wear debris and micro-contact maintains the cubic structure because it is quenched on leaving the contact. The contact pressure is sudden a way and the high specific surface of the small debris reduces the temperature over radiation and heat transfer.

5 Conclusions

The overlap ratio has an important influence on self-mated ZrO_2 sliding couples. The rotating specimen (overlap ratio 2%), owing to the cyclic, thermal loading, shows higher wear than the stationary specimen (overlap ratio 100%). At 0·1 m/s, nearly all rotating-specimen wear is in the high-wear region.

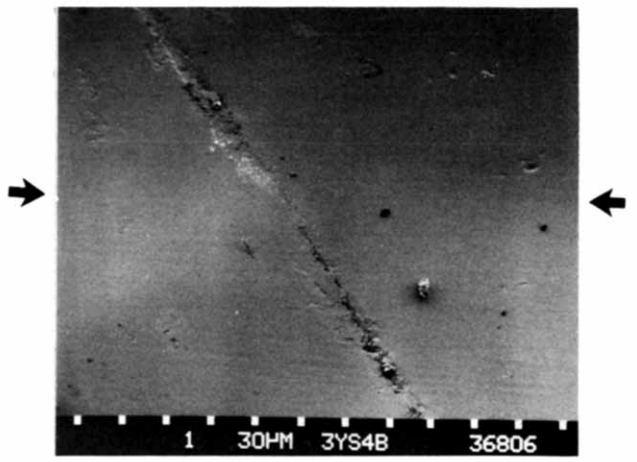

Fig. 12a. Wear track of 3 Y–ZrO_2 in the low-wear region ($T = 22°C$; $v = 0{\cdot}04$ m/s).

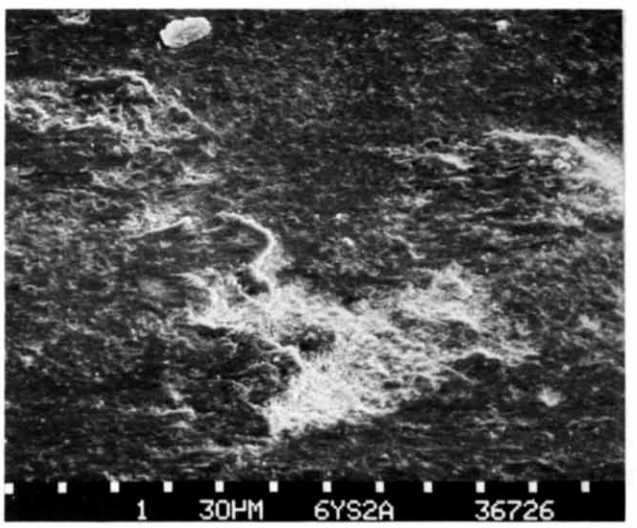

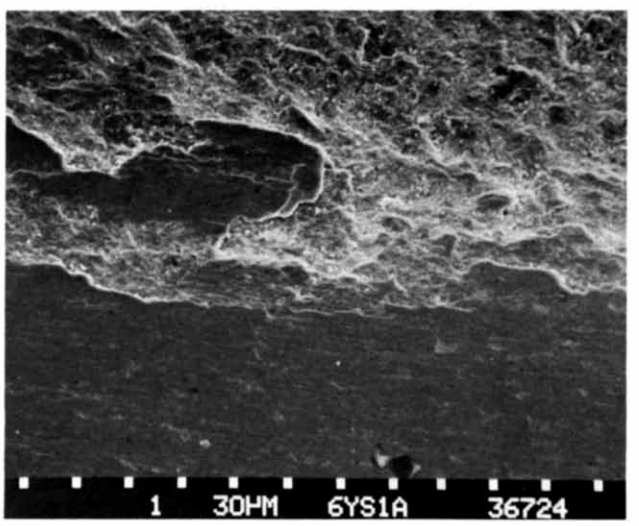

Fig. 12b. Wear track of 6 Y–ZrO_2 at 22°C (above: low wear; $v = 0{\cdot}1$ m/s; below: high wear; $v = 3{\cdot}38$ m/s).

The low-wear–high-wear transition during the increase in sliding velocity and at ambient temperature is a function of the phase composition and of the stabilizing oxide. Under high contact pressures and low sliding velocities, the tetragonal material ZrO_2 ($2Y_2O_3$) has the highest wear resistance as a sliding partner with 100% overlap ratios.

MgO–ZrO_2 with the special duplex structure has the best wear performance. In the medium speed range, where thermal effects become tribologically important, the cubic ZrO_2 phase, as thermodynamically stable material, has the lowest wear for the pin (100% overlap ratio) because this phase cannot transform under the high flash temperatures and pressures in the micro-contact into the cubic phase.

From these results it can be concluded that the low-wear–high-wear transition of the tetragonal ZrO_2 stationary specimen can be shifted to higher speeds by using rotating materials with high thermal conductivities ($100\ W/m\ K < \lambda < 180\ W/m\ K$), like AlN and SiC[20,21] (see Fig. 4). The carbide materials withstand thermal cyclic loadings better because of their physical properties, and at the same time the hot-spot temperature of the ZrO_2 stationary specimen is reduced.

Owing to the ionic bonding of ZrO_2 and the possibility of adsorbing polar H_2O, the coefficient of friction can be as low as 0·1 at start-up.

Under steady-state conditions, the coefficient of friction in closed tribosystems under solid-state friction is between 0·4 and 1·0.

The wear coefficient of self-mated MgO–ZrO_2 couples increases significantly with increasing sliding speed and ambient temperature. Frictional heating is enhanced by increasing velocity, and ambient temperature may have the same effect.

The low-wear–high-wear transition is associated with the formation of the cubic phase from the initial monoclinic and tetragonal phases.

Acknowledgement

The authors acknowledge the financial support of the BMFT (German Ministry Research and Technology).

References

1. Woydt, M. & Habig, K.-H., Technisch-physikalische Grundlagen zum tribologischen Verhalten kermischer Werkstoffe. BAM-Forschungsbericht FB 133,2. Auflage 1988; N & W Verlag, D-2850 Bremerhaven.
2. Czichos, H. & Woydt, M., Entwicklungstendenzen tribotechnischer Werkstoffe für den Fahrzeugbau. *Automobiltechnische Zeitschrift*, **90** (1988) 237–46; 415–21.
3. Griffion, J. A., Blair, S. & Winer, W. O., Infrared surface temperature measurements in a sliding ceramic–ceramic

contact. In *Proceedings of the Leeds–Lyon Symposium on Tribology*, Butterworth Publishing, Guildford, UK, 1985.
4. Yust, C. S., Oak Ridge National Laboratory, PO Box X, Oak Ridge TN 37381, USA, 1988, pers. comm.
5. Hwand, B., Houska, C. R., Ice, G. E. & Habenschuss, A., X-Ray analysis of the near surface phase distribution of the wear on a PSZ disc. *Adv. Ceram. Mater.*, **3** (1988) 180–3.
6. Breunig, B., Aerodynamische Federlager für hohe Drehzahlen und hohe Temperaturen. Dissertation, Universität Karlsruhe, FRG, 1986.
7. Fischer, T. E., Anderson, M. P. & Jahanmir, S., Friction and wear of tough and brittle zirconia in nitrogen, air, water, hexadecane and hexadecane containing stearic acid. In *Proceedings of International Conference on Wear of Materials*, Houston, Texas, USA, 1987, ed. K. C. Ludema, p. 242.
8. Gane, N. & Breadsley, R., Measurement of the friction and wear of PSZ and other hard materials using a pin on disc machine. Paper presented at International Tribology Conference, Melbourne, Australia, 2–4 December 1987.
9. Gienau, M., Woydt, M. & Habig, K.-H., Hochtemperatur-tribometer für Reibungs- und Verschleiß- untersuchungen bis 1000°C. *Materialprüfung*, **29** (1987) 197.
10. Woydt, M. & Habig, K.-H., Influence of temperature and sliding speed on friction and wear of SiSiC and $MgO–ZrO_2$. *Ceram. Sci. Engng Proc.*, **9** (1988) 1419–31.
11. Dworak, U., Olapinski, H. & Burger, W., Dilatation behaviour of two differently heat-treated commercial magnesia partially stabilized zirconias. *J. Amer. Ceram. Soc.*, **69** (1986) 578.
12. Woydt, M. & Habig, K.-H., Tribological behaviour of fine ceramics in screening test and applications up to 1000°C. *Metall*, **43** (1989) 218.
13. Tönshoff, H. K. & Bartsch, S., Thermal load simulation by laser-beaming, *Ceram. Sci. Engng Proc.*, **9** (1988).
14. Meyer, B., Tönshoff, H. K. & Bartsch, S., Einfluß thermischer Belastungen auf das Verschleißverhalten keramischer Schneidstoffe. *VDI-Berichte Nr. 670*, Band II, 1988.
15. Kuhlmann-Wilsdorf, D. & Makkel, D., (University of Virginia, Dept. of Material Science, 304 Physics Building, Charlottesville, VA 22901, USA), 1988, 1989, pers. comm.
16. Kuhlmann-Wilsdorf, D., Makkel, D. D. & Sondergard, N. E., Refinement of flash-temperature calculations. Paper presented at International Conference on Engineered Materials for Advanced Friction and Wear Applications, ASM Int., 1–3 March 1988.
17. Griffion, J. A., Bair, S. & Winer, W. O., Infrared surface temperature measurements in a sliding ceramic–ceramic contact. In *Proceedings of the Leeds–Lyon Symposium on Tribology*, Butterworth Publishing, Guildford UK, 1985.
18. Liu, L.-G., New high pressure phase of ZrO_2 and HfO_2 *J. Phys. Chem. Solids*, **41** 331–4.
19. Michel, D., Mazerolles, L. & Perez Y Jorba, M., Fracture of metastable tetragonal zirconia crystals. *J. Mater. Sci.*, **18** (1983) 2618–28.
20. Habig, K.-H. & Woydt, M., Tribologisches Hochtemperaturverhalten keramischer Werkstoffe unter Festkörpergleitreibungsbedingungen. *VDI-Berichte Nr. 670*, 1988, p. 683.
21. Woydt, M. & Habig, K.-H., High-temperature tribology of ceramics. *Tribology Int.*, No. 22 (1989) 75–88.
22. Woydt, M., Einfluß von Temperatur und Gleitgeschwindigkeit auf Reibung und Verschleiß ZrO_2 Gleitpaarungen. Ph.D. Thesis, Technical University of Berlin, Berlin, FRG, 1989.